NASA-CR-203983

021647

THE MEASUREMENT OF SULFUR OXIDATION PRODUCTS AND THEIR ROLE IN HOMOGENEOUS NUCLEATION

NASA Grant No. NAGW-4692
Georgia Tech Project No. A-5036

Progress Report/Request for Incremental Funding
April 1, 1996—March 31, 1997/July 1, 1997—June 30, 1998

Submitted to:

NASA Headquarters
Washington, DC 20546

Attn: Dr. R. A. Schiffer

Submitted by:

Electro-Optics and Environmental Materials Laboratory
Georgia Tech Research Institute
Georgia Institute of Technology
Atlanta, GA 30332

Principal Investigator: Dr. F. L. Eisele

ANNUAL PROGRESS REPORT

Over the past year, progress has been made on this project in a variety of areas. One major thrust has been to investigate the formation of neutral sulfuric acid dimers using a Selected Ion Chemical Ionization Mass Spectrometer (SICIMS) and a new ion source/reactor constructed for this project. The latter, recently developed source allows the application of selected ion chemical ionization at atmospheric pressure and for ion reaction times which can be varied from 1 to 100 ms. This wide range of reaction times is important because it provides a means of separating ion induced molecular ion clusters from those which result from proton exchange with a pre-existing neutral H_2SO_4 cluster. In the absence of neutral H_2SO_4 dimers or trimers, $HSO_4^- \cdot (H_2SO_4)_n$ ions (with $n > 0$) will still form in the presence of gas phase H_2SO_4 by successively incorporating H_2SO_4 molecules onto HSO_4^- ions until some steady state value of n is reached. The latter $HSO_4^-(H_2SO_4)_n$ ions (which will be called ion-induced clusters) are indistinguishable from those resulting from H_2SO_4 dimers or trimers which loose a proton to some initial reactant ion. Thus, $HSO_4^- \cdot (H_2SO_4)_n$ ions which are being used to investigate neutral H_2SO_4 cluster formation have at least two sources:

$$NO_3^- + H_2SO_4 \rightarrow HSO_4^- + HNO_3 \qquad (1a)$$

$$HSO_4^- + H_2SO_4 + m \rightarrow HSO_4^- \cdot H_2SO_4 + m \qquad (1b)$$

$$HSO_4^- \cdot (H_2SO)_{n-1} + H_2SO_4 + m \rightarrow HSO_4^- \cdot (H_2SO_4)_n + m \qquad (1c\text{-}n)$$

and $$NO_3^- + (H_2SO_4)_n \rightarrow HSO_4^-(HSO_4)_{n-1} + HNO_3 \quad (2)$$

Reaction 1 is a multi-step reaction in which the ratio of $\left[HSO_4^- \cdot (H_2SO_4)_{n-1}\right]/\left[HSO_4^-\right]$ is dependent on $[H_2SO_4]$ and reaction time. In contrast, reaction 2 is simply a proton exchange reaction between any of the $(HSO_4)_n$ clusters and NO_3^-, and the ratio of $\left[HSO_4^- \cdot (H_2SO_4)_{n-1}\right]/\left[HSO_4^-\right]$ should not decrease rapidly as reaction time is shortened. Thus, if the $\left[HSO_4^- \cdot H_2SO_4\right]/\left[HSO_4^-\right]$ ratio is plotted as a function of time for short reaction times as shown in Figure 1, a linear plot would be expected for the latter ratio if $HSO_4^- \cdot H_2SO_4$ were formed solely by an ion induced process. Figure 1 shows data obtained using the recently constructed 1-100 ms ion source/reactor apparatus. The approximately linear time dependence is expected at the relatively long reaction times shown, because under such conditions ion-induced cluster formation is known to be important. At even long times, the ratio of $\left[HSO_4^- \cdot H_2SO_4\right]/\left[HSO_4^-\right]$ must eventually become time independent at some equilibrium concentration ratio. As the reaction time is decreased, however, if $(H_2SO_4)_2$ exists and reacts with NO_3^- (which it is expected to), then the slope of the line in Figure 1 is expected to approach a constant in which the ratio of $\left[(H_2SO_4)_2\right]/[H_2SO_4]$ is represented by $\left[HSO_4^- \cdot H_2SO_4\right]/\left[HSO_4^-\right]$ times some relative reaction rate constant for $NO_3^-/(H_2SO_4)_2$ and NO_3^-/H_2SO_4. Therefore much of our efforts have gone into trying to measure this ratio under near ambient conditions and at the shortest possible reaction times. The near linear dependence of the ratio (even down to the 1 ms time scale) suggests that less than 1% of the gas phase H_2SO_4 molecules are dimers, even at the extreme cases of -20°C and $[H_2SO_4]$ = 100 pptv shown in Figure 1. Thus, at

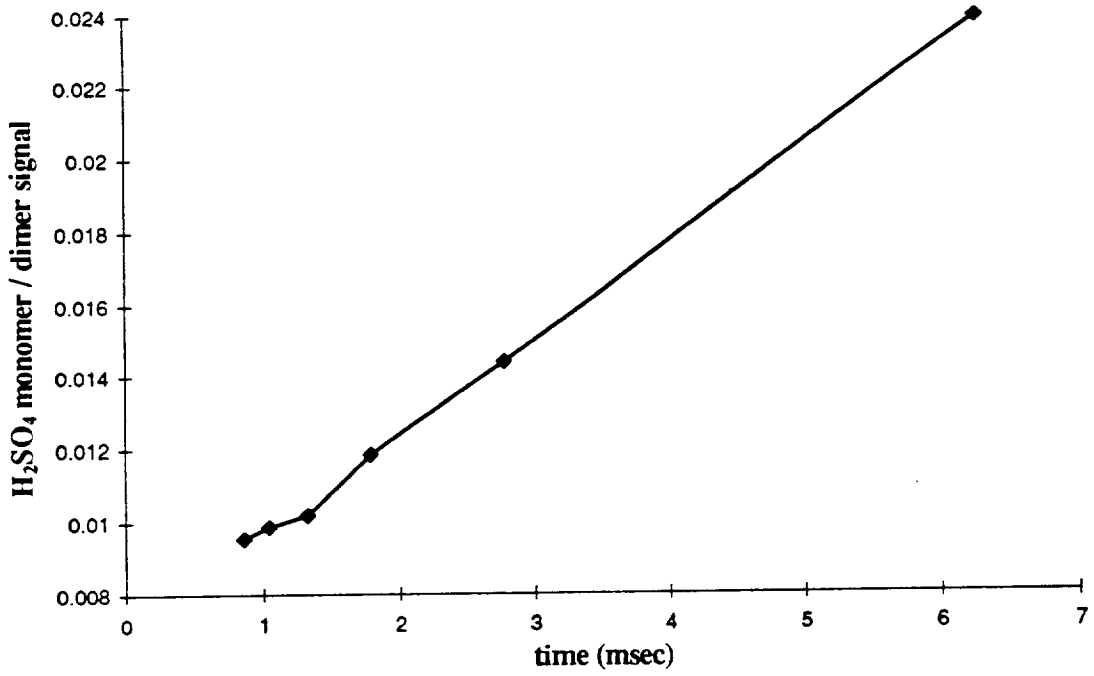

Figure 1. Measurement of the ratio of H_2SO_4 monomers to dimer as a function of time at -20°C.

temperature and [H_2SO_4] more typical of previous field studies where nucleation events have been observed, the percentage of $(H_2SO_4)_2$ clusters present would probably be expected to be orders of magnitude lower still. While this does not rule out the role of H_2SO_4 dimers and trimers in particle nucleation it does make it seem far less likely that a sufficient number of these clusters exist, and that they will react fast enough with NH_3 to control tropospheric nucleation. As a consequence of these laboratory studies, the most likely tropospheric nucleation mechanism would now appear to be the gas phase reaction of NH_3 with H_2SO_4 (rather than with H_2SO_4 dimers) to form ammonium bisulfate molecules and their subsequent formation of clusters. The present study has caused us to reconsider the relevance of a previous experimental laboratory investigation aimed at determining the potential interference of NH_3 in H_2SO_4 measurements. We may already have some evidence suggesting that while NH_3 does not react quickly with H_2SO_4 in the gas phase, it may, in fact, react slowly. Determining the extent to which NH_3 and H_2SO_4 react to form ammonium bisulfate is, thus, becoming of much greater importance (see work being proposed section).

Other areas of progress include measurements of the accommodation coefficient of H_2SO_4 on ammonium sulfate, sodium chloride and other particles surfaces. These measurements were made in our laboratory in conjunction with colleagues from the University of Minnesota. The accommodation coefficient for H_2SO_4 is important not only for understanding the growth of CN in CCN, but it is also used to calculate the flux of nucleating particles from measured ultrafine particle distributions. Since literature values of this coefficient vary by nearly 2 orders of magnitude (0.02-1.0), and we had the ability to make the first direct measurement of these parameters, it seemed like a worthwhile project. The accommodation coefficients were found to be 0.73 ± 0.21 and 0.80 ± 0.23 for ammonium sulfate and sodium chloride respectively. The details of this very successful

measurement have recently been submitted for publication, and are included in Appendix A.

Progress has also been made on testing new ion reaction schemes for measuring NH_3 in the field. In the first year of this grant, several ions were tested in the laboratory as possible candidates for the reactant ion to be used for measuring NH_3 in the atmosphere. This year, an approximately 1 month long local field study was conducted, in which two reactant ions were tested for use in measurements of ambient NH_3 and various hydrocarbons by SICIMS. One of the compounds tested was acetone, which was previously used in some of last year's laboratory tests. A second compound used to generate reactant ions was ethanol, which had not been tested previously, but which looks very encouraging. Both compounds readily form ions by attaching a proton, and both also readily form clusters with themselves. In the case of ethanol the most common cluster ion $C_2H_7O^+ \cdot C_2H_6O$ still appears to react quickly with NH_3 via proton exchange to form NH_4^+ and $NH_4^+ \cdot C_2H_6O$. Figure 2 shows the initial ethanol reactant ion distribution in ambient air which is dominated by $C_2H_7O^+ \cdot C_2H_6O$, but which also contains a small peak of the core ion $C_2H_7O^+$. The NH_4^+ and $NH_4^+ \cdot C_2H_6O$ peaks are a result of reactions of $C_2H_7O^+ \cdot (C_2H_6O)_n$ for n=0,1 with ambient NH_3 at a field site a few km north of the NCAR Mesa Laboratory Building at the edge of the foothills of the Rocky Mountains. Air flow at this site is typically from the west and is relatively clean during the morning hours. At some point during late morning or early afternoon, the flow will typically switch to a more easterly (or sometimes northerly and southerly) component, which brings up air from the city of Boulder, Denver, or farming areas to the east. Figure 3 shows an initial test of the new SICIMS ammonia measurement technique used at this site. Figure 3 also shows the wind direction during this same time period. As is typical of this site, prevailing westerlies bring down relatively clean air from the mountains which, as seen from Figure

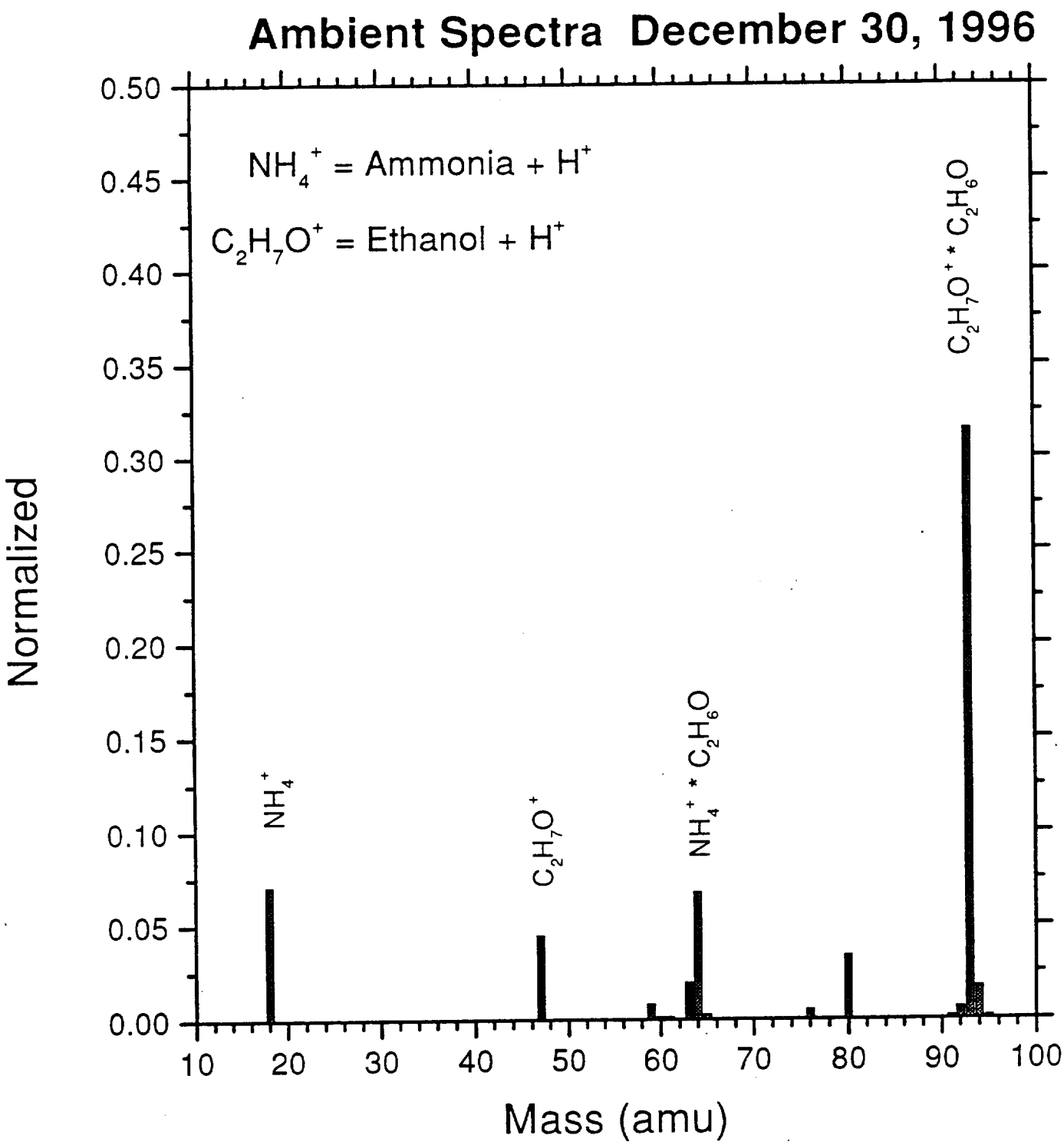

Figure 2. Typical ion spectrum measured during a recent field study showing nearly exclusively reactant and production peaks.

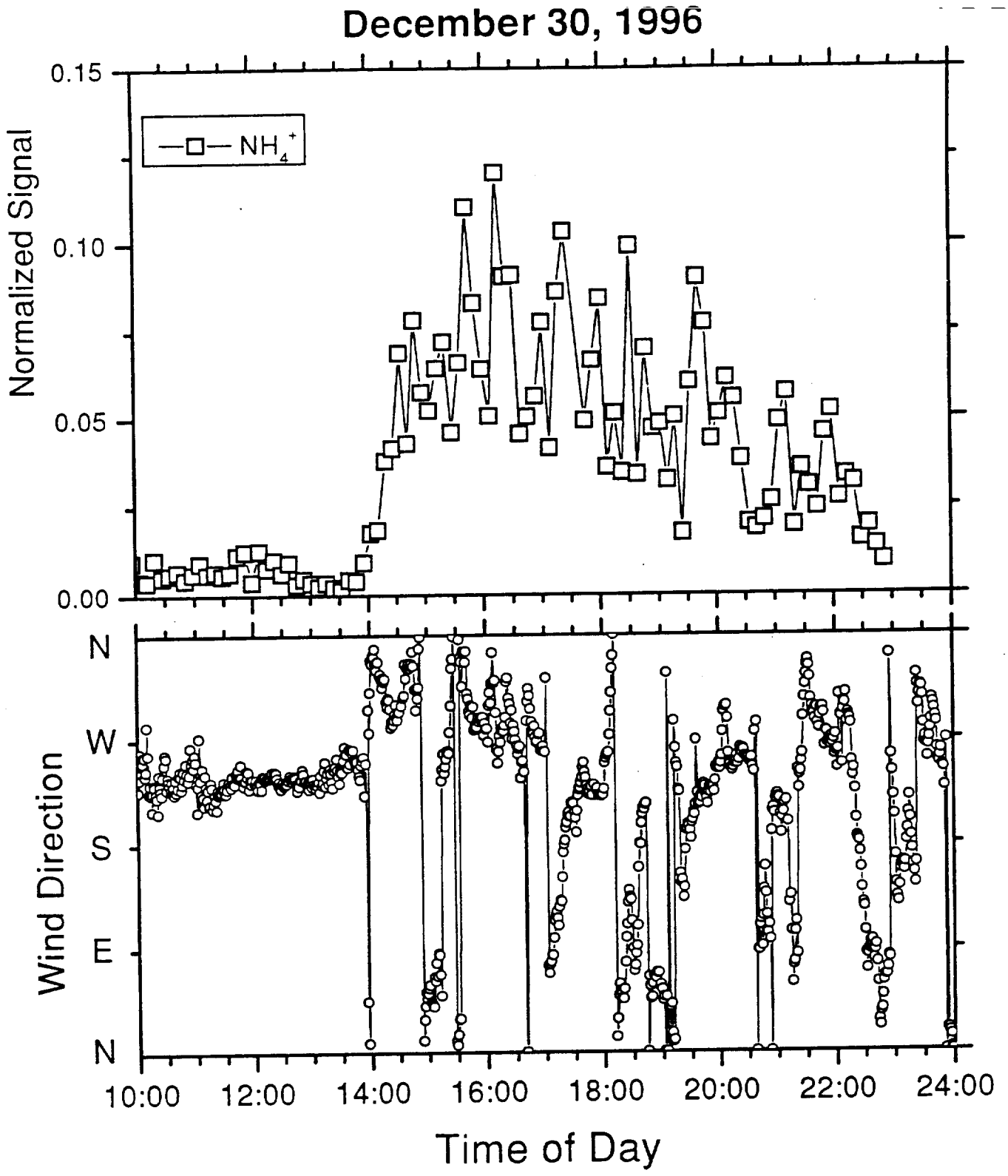

Figure 3. Preliminary measurements of NH_3 and wind direction as a function time of day.

3, contains little NH_3. In early afternoon at about 14:00 hours, the wind switches direction abruptly and its velocity drops. The air mass present after 14:00 is probably from urban and farm areas and would be expected to contain far more NH_3, which agrees well with the observations shown in Figure 3. Thus far, only very preliminary tests of this new technique have been performed, but the results look quite promising, particularly since the area in which these measurements were made contains large amounts of hydrocarbons which could have had a much larger than observed interference. For measurements in marine environments, $C_2H_7O^+$ can probably be used to measure NH_3, and DMSO (and perhaps $DMSO_2$ as well) with the same ion source.

Work Proposed for the Next Year of This Project

A series of measurements are proposed to assess the role of gas phase reactions of NH_3 with H_2SO_4 monomers as a mechanism for nucleating particles. Since neither ammonium bisulfate nor ammonium sulfate are likely to be directly ionized using selected ion chemical ionization, an indirect means of investigating NH_3/H_2SO_4 reactions and cluster formation is proposed. First, a flow tube measurement of the rate of loss of gas phase H_2SO_4 will be made via SICIMS as a function of NH_3 concentrations. A previous test suggests that this rate coefficient should be measurable using the present technique. Next the expected ammonium bisulfate product will be searched for as an ion cluster associated with HSO_4^- or NO_3^- ions. These clusters will probably be very weakly bound and thus, particular caution must be exercised during their sampling into the vacuum analysis region. As clusters of ammonium bisulfate and H_2O grow larger, they are even more likely to be associated with a charge. Thus $(HNH_4SO_4)_2(H_2O)$ clusters which might well be the critical cluster responsible for nucleation will be studied by charging via selected ions and subsequently detected by mass spectrometry and/or tandem mass

spectrometry (we are presently switching from a standard mass spectrometer to a tandem mass spectrometer due to the increased complexity of the reactions under investigation).

In addition to nucleation studies, the development of new SICIMS measurement schemes are also planned. Ions such as $C_2H_7O^+$ show much promise for making possible measurements of compounds such as NH_3, DMSO, and quite possibly DMS and $DMSO_2$ as well with a single ion source. Thus, these and similar reaction schemes for other DMS oxidation products will continue to be a major focus of the present project.

Measurements of the H_2SO_4 Mass Accommodation Coefficient onto Polydisperse Aerosol

A.Jefferson[1], F.L. Eisele[1,2]
P.J. Ziemann[3], J.J.Marti[4], R.J. Weber[5] and P.H. McMurry[6]

1) Atmospheric Chemistry Division
National Center for Atmospheric Research
Boulder, CO

2) Georgia Tech Research Institute
Georgia Institute of Technology
Atlanta, GA

3) Statewide Air Pollution Research Center and
Department of Soil and Environmental Sciences
University of California, Riverside
Riverside, CA

4) Naval Research Laboratory
Washington, D.C.

5) Enviromental Sciences Laboratory
Brookhaven National Labs
Department of Energy
Upton, N.Y.

6) Particle Technology Laboratory
Department of Mechanical Engineering
University of Minnesota
Minneapolis, MN

Submitted Journal of Geophysical Research, January 1997

Abstract

The loss rate of H_2SO_4 vapor onto submicron aerosols was measured for three different aerosol substrates. The experimental technique involved direct flow tube measurements of H_2SO_4 decay rates onto a polydisperse aerosol using chemical ionization mass spectroscopic detection. The aerosols of this study were partially hydrated crystalline salts with diameters in the size range of 20 to 400 nm. The mass accommodation coefficients, α, were calculated from the first order rate constants for H_2SO_4 loss to be 0.73 ± 0.21, and 0.80 ± 0.23 for loss onto $(NH_4)_2SO_4$ and NaCl, respectively. Measurements of the loss rate of H_2SO_4 onto a NaCl aerosol coated with stearic acid resulted in lower mass accommodation coefficients with values of 0.31 and 0.19 for aerosol with high and low stearic acid coverage, respectively. The observed decrease in α on an aerosol with a hydrocarbon coating suggests that aerosol composition is a key factor in H_2SO_4 adsorption on to a particle surface.

Introduction

Aerosols have a significant impact on climate forcing by their ability to scatter solar radiation and increase cloud albedo, which result in a cooling of the lower troposphere [Penner et al.,1995, Wigley and Raper, 1992]. The magnitude of this effect depends in part on the aerosol microphysical properties, particularly the particle composition, size and number density [Schwartz, 1996]. Sulfates, along with nitrates and organics, form the primary constituents of submicron condensation nuclei (CN) which scatter short wave radiation and which can grow to form cloud droplets. The formation and initial growth of CN are thought to proceed through bimolecular nucleation of H_2O and H_2SO_4 and subsequent uptake of gas phase H_2SO_4 onto the particle surface [Kriedenweis et al., 1991]. An unknown parameter needed to quantify CN nucleation and growth rates is the mass accommodation coefficient of H_2SO_4 onto particles.

Current models of aerosol nucleation rates are especially sensitive to the H_2SO_4 mass accommodation coefficient, α. Estimates of α range between 0.02 and 1.0. In their model of bimolecular nucleation rates Pandis et al.[1994] calculated a 45 percent reduction in the H_2SO_4-H_2O nucleation rate when α was changed from 0.02 to 0.05. Nucleation rates modeled by Kulmala et al.[1995] show a similar strong dependence on α. In laboratory measurements of aqueous H_2SO_4 particle growth, Van Dingenen and Raes [1991] determined a value for α between 0.02 and 0.09. Alternatively, two field studies, which measured steady state H_2SO_4 production rates [Eisele and Tanner, 1993, Weber et al.,1996], found that values for α of 0.5 and 1.0, respectively gave good agreement with their data.

Submicron aerosol composition may vary between remote or polluted and marine or continental environments. Aerosols from remote marine environments were found to contain mostly SO_4^{2-}, $CH_3SO_3^-$ and NH_4^+ ions, while larger sea salt aerosols also contain Na^+ and Cl^- ions [Huebert et al.,1996, Savoie et al., 1993]. In addition, aerosols found in continental and anthropogenically influenced air masses may contain considerable amounts of organics [Saxena et al., 1996, Novakov and Penner, 1993]. As the substrate composition varies so too may the uptake of H_2SO_4. As an acid, H_2SO_4 would seem likely to bond most strongly with substrates containing polar or basic binding sites.

Here, we present measurements of the mass accommodation coefficient of H_2SO_4 onto aerosols composed of $(NH_4)_2SO_4$, NaCl and NaCl coated with stearic acid. This study is the first measurement of the gas phase H_2SO_4 uptake rate onto aerosols which directly measured changes in the gas phase H_2SO_4 concentration. The aerosol uptake experiments in this study make use of the sensitive technique of selected ion chemical ionization mass spectrometry (SI/CIMS) to measure the removal rate of H_2SO_4 by aerosols. In this study H_2SO_4 concentrations in the range of 0.1-10 pptv were measured at a relative humidity at or below 11 percent. Measurements at a higher relative humidity, representative of the lower troposphere, were hindered by the low equilibruim vapor pressure of H_2SO_4 above the acid solution source used in these experiments. Possible changes in the H_2SO_4 mass accommodation coefficient with ambient conditions such as relative humidity and aerosol composition are discussed.

Experimental

Polydisperse aerosols were generated by atomizing aqueous solutions of either $(NH_4)_2SO_4$ or NaCl. Filtered nitrogen was used as a carrier gas for the aerosol flow at a flow rate of about 1.24 liters min^{-1}. The aerosol droplets passed through a silica gel diffusion dryer before joining the humidified nitrogen carrier flow at the entrance of the flow tube injector. Particle sizes ranged in diameter from 20 to 400 nm. In the experiments involving stearic acid coated aerosols, NaCl particles were coated with stearic acid by passing the aerosol flow through a heated 6 " long glass tube containing both solid stearic acid and its vapor. The thickness of the acid coating on the particles was controlled by adjusting the temperature of the glass tube and thus the stearic acid vapor pressure. The tube was heated to 104° and 88° C for high and low particle coatings of stearic acid. The aerosol flow made up about 5 percent of the total gas flow.

Aerosol surface areas were determined from particle size distributions measured using a scanning electrical mobility spectrometer (SEMS) [Wang and Flagan,1990]. The instrument consists of a particle charger, a differential mobility analyzer (DMA), a condensation nucleus counter (CNC) and SEMS software for rapid scanning of the particle size distribution. Sampled particles were charged to near-Boltzmann equilibrium by a ^{210}Po source. The particles then passed through a DMA, which separated particles by their electrical mobility, allowing only those with mobilities in a narrow selected range to exit to the CNC detector. The particle mobility distribution was measured by scanning through the particle size range, typically 20 nm to 400 nm in diameter. For spherical particles, whose size is precisely defined by the diameter, the particle size distribution can be accurately calculated from the mobility distribution.

In our experiments, aerosol was sampled from the downstream end of the flow tube reactor and diluted with filtered, dry nitrogen (~1:6) in order to maintain particle concentrations in the instrument range. The aerosol flow rate into and out of the DMA was 1.0 liters min^{-1}, the DMA sheath air flow rate was 7.3 liters min^{-1} of filtered room air and the CNC flow rate was 1.5 liters min^{-1}, of which 1.0 liters min^{-1} was aerosol from the DMA, the remainder being filtered room air. The use of filtered room air for the DMA sheath flow should have no effect on the measured particle size distribution since the ambient relative humidity was well below the deliquescence point of both NaCl and $(NH_4)_2SO_4$.

The particle size distributions used for our calculations of aerosol surface areas were corrected for particle charging and losses in the DMA using the method of Hagan and Alofs [1983]. No correction for CNC counting efficiency was required since the aerosol surface area was associated with sizes that are detected with near 100 % efficiency. The flow was laminar in the flow tube and tube leading to the DMA, making particle losses by diffusion neglible. Aerosol surface areas were calculated by assuming that the particles were spherical, which is approximately true for $(NH_4)_2SO_4$ [Kelly and McMurry, 1992] although not for NaCl. Nonetheless, because NaCl particles are apparently cubic [Lodge and Tufts, 1955], and the ratio of the side length of a cube to its mobility diameter is 0.746 [Dahneke, 1973], the surface area for a sphere and a cube with the same mobility diameters differ only by ~6 %. Typical aerosol surface areas per cm^{-3} for these experiments were 600 $\mu m^2 cm^{-3}$.

Flow Tube Apparatus

The reaction tube for measurement of kinetic decay rates consisted of a jacketed pyrex flowtube, 80 cm in length with a 7.6 cm inside diameter. A moveable, 2.5 cm diameter pyrex injector was mounted inside the flow tube. The injector diameter reduces to a small orifice about 5 cm before its exit. After this constriction the injector flares to nearly the full diameter of the flow tube and has a stainless steel, fine mesh screen attached on the end. The H_2SO_4 vapor source consisted of a small cap containing a concentrated H_2SO_4 solution which rested on top of the injector end screen. The injector design ensured that the aerosol flow turbulently mixed with H_2SO_4 vapor in this region between the constriction and injector exit and that the total gas flow was evenly distributed across the flow tube diameter. A schematic diagram of the experimental setup is given in Figure 1.

The H_2SO_4 concentration in the flow gas depended on the equilibruim vapor pressure of H_2SO_4 above the acid solution source and as such varied strongly with the relative humidity of the gas flow. At relative humidities above 10% the H_2SO_4 vapor pressures of sulfuric acid solutions drop below 10^{-9} torr [Ayers et al., 1980, Marti et al., 1997], which resulted in H_2SO_4 concentrations too low to measure an accurate decay. The present measurements were limited to a relative humidity between 11 and 0.3%.

The temperatures of both the flow tube and the humidified carrier gas were maintained at a constant 25 ° C. A humidified air stream was generated by flowing N_2 gas through microporous PTFE tubing immersed in deionized and distilled water. This air stream then flowed through a heat exchanger before combining with the aerosol flow in the injector tube entrance. Water from a temperature controlled bath was circulated through both the external flow tube jacket and the gas heat exchanger. The gas temperature was measured

by a thermocouple at the flow tube exit. The relative humidity of the carrier gas was measured at the flow tube exit by a dewpoint monitor.

CIMS detection of H_2SO_4

The decay in the H_2SO_4 concentration as a function of injector position was measured using the technique of selected ion chemical ionization mass spectrometry (SI/CIMS). This technique involved sampling the gas from the center of the flow tube into a chemical ionization source. After merging with the ions from this source, the gas flowed through a reaction region where H_2SO_4 in the flow gas underwent a proton exchange reaction with NO_3^- and was converted to HSO_4^-. The reactant and product ions were then focused into a mass spectrometer and detected. The relative H_2SO_4 concentration is given as the ratio of the HSO_4^-/NO_3^- ion signals. Two steps were taken to assure that hydrates of H_2SO_4 were detected along with the monomer. Before entering the mass spectrometer the ion containing gas was directed through a flow of dry nitrogen gas, which acted to dehydrate the ions. Next the ions passed through a small aperture into a collision dissociation region. A voltage held across the vacuum chamber accelerated the ions and induced collisions with the background nitrogen gas strong enough to dissociate any remaining ion clusters. Thus, hydrates of HSO_4^- were converted to the monomer sulfate ion and detected with the same efficiency. Further details of the CIMS instrument can be found in prior publications [Eisele and Tanner 1991, 1993, Tanner and Eisele, 1995 and Tanner et al.,1996].

Flowtime measurements

At a flow rate of 23.5 liters min^{-1} and a Reynold's number of 650 typical of the present experiment, the gas in the flow tube shown in Figure 1 is expected to develop a laminar flow profile with some radial and axial diffusion. However, to promote a short ion-molecule reaction time, the flow in the CIMS sample inlet was considerably faster than that in the main flow tube, and as a result the flow accelerated, permitting a radial convergence of the gas in the flow tube into the sample inlet. Rather than assume laminar flow conditions, a direct measurement of the flowtime was made using a pulsed ion source. A corona discharge ion source was constructed by running a wire down the center of the injector to a distance within 2-3 cm of the end metal screen which was held at electrical ground so that the flow tube remained a near field free region. A counter card triggered a 5 kv, 10 ms wide electrical pulse to induce the corona discharge and also initiate computer data collection. Data was collected in 10 second cycles with 0.2 second time steps. The flow times were calculated using a weighted average of the signal counts at each time step. Figure 2 shows the linear fit of the flow times with respect to laminar flow. The flow time is best fit by the equation

$$\text{time (sec)} = 0.0639\,x + 0.3715 \qquad (1)$$

where x is the injector position in cm from the top of the CIMS sample inlet tube.

Unlike a neutral gas, a positively charged ion flow is subject to space charge repulsions which acts to accelerate the ions thereby increasing the diffusivity of the ions beyond that of neutral molecules. Increased ion diffusivity results in a broader time profile and shifts the measured residence time of the ion to times longer than those of the neutral molecule. Under the flow conditions of these experiments, the CIMS instrument sampled about 18

percent of the flow tube area. An ideal laminar flow with no radial or axial diffusion would result in an average flow rate of time (sec) = 0.0616 x. The difference between this flow rate and the measured value of 0.0639 x given in equation 1 is due to diffusional broadening of the time profile. The time offset of 0.3715 seconds in equation 1 reflects the time needed for the ions to travel from a relative zero position on the flow tube to registering an ion signal on the computer. The small difference in the ideal laminar flowrate and the measured ionic flow rate indicates that the difference between the radial and axial diffusion of the ions and neutral molecules is small for the low ion concentrations of these experiments and has a negligible effect on the measured flow times. The exponential fits of the experimental decays used a value for the reaction time given by equation 1.

Reaction kinetics and mass transport

The loss of H_2SO_4 onto an aerosol surface follow pseudo first order kinetics provided the aerosol number density and uptake ability remain constant during the course of a single measurement. Changes in the H_2SO_4 concentration with injector position can be expressed as

$$\frac{d[H_2SO_4]}{dt} = -K[H_2SO_4] \qquad (2)$$

where $K = k_1 + k_d$. Here k_1 is the pseudo first order rate constant for loss of H_2SO_4 onto aerosol and k_d is the background decay constant for diffusion and wall losses of H_2SO_4.

A determination of k_1 will depend on the mass transport between H_2SO_4 and the particles. The particles generated in these experiments are between 20 and 400 nm in

diameter and fall in the transition regime between gas kinetic and diffusion limits for mass transport. For uptake onto a monodisperse aerosol the first order rate constant can be calculated in terms of a mass accommodation coefficient, α, with the Fuchs-Sutugin equation [Fuchs and Sutugin, 1970].

$$k_1 = \frac{\alpha N_p c \pi D^2}{4(1+\alpha B)} \qquad (3)$$

where $$B = \frac{(0.75+0.283Kn)}{Kn(Kn+1)} \qquad (4).$$

From the above, N_p is the particle number density, c is the mean molecular speed, D is the particle diameter and Kn is the Knudsen number which is function of the molecular diffusivity, D_g, and particle size: $Kn = 6D_g/cD$. Here, the mass accommodation coefficient represents the number of H_2SO_4 molecules reversibly adsorbed onto the particle surface per gas kinetic collision.

For a polydisperse aerosol distribution, the observed k_1 is the integral with respect to the particle diameter, D, of the size dependent psuedo 1st order rate constant for H_2SO_4 loss on the aerosol, i.e.

$$k_1 = \int k_1(D)dD \qquad (5)$$

Numerically integrating over D the following equation is obtained

$$k_1 = \sum_i \frac{\alpha c \pi D_i^2 \frac{dN}{d\ln D_i}}{4(1+\alpha B_i)} \Delta \ln D_i \qquad (6)$$

The aerosol number concentration for each particle diameter, $\frac{dN}{d\ln D}\Delta \ln D$, was calculated as an average of all of the size distributions recorded at various injector

positions for a given decay. Calculation of the mass accommodation coefficient involved iteratively changing α in the equation for k_1 until the calculated value of k_1 equaled the measured value.

The diffusion coefficient, D_g, of H_2SO_4 in N_2 was chosen to be 0.1 ± 0.02 cm^2 s^{-1} in accordance with prior calculations (Roedel, 1979, Marti et al., 1996) and adjusted for an ambient pressure of 615 torr. In a humid air flow a fraction of the H_2SO_4 molecules are hydrated and have a lower effective diffusivity. However, at the low relative humidities of these experiments most of the H_2SO_4 molecules were unhydrated or monohydrated. The small decrease in diffusivity of the monohydrate relative to H_2SO_4 is expected to be well within the uncertainty in the value of D_g (Marti et al., 1997).

Results

The first order decay of H_2SO_4 onto an aerosol surface was measured for submicron polydisperse particles composed of $(NH_4)_2SO_4$, NaCl and NaCl coated with stearic acid. Figure 3 shows the H_2SO_4 signal versus injector position for different concentrations of NaCl aerosol. The measured first order rate constants and calculated values of the mass accommodation coefficient along with the uncertainties are given in Table 1 for H_2SO_4 loss onto each of the substrates. The mass accommodation coefficients for H_2SO_4 loss onto $(NH_4)_2SO_4$ and NaCl aerosol were found to be 0.73 ± 0.21 and 0.80 ± 0.23, respectively. The measurement uncertainties are given as 2σ, twice the standard error for each set of measurements. The measured mass accommodation coefficients for H_2SO_4 uptake onto NaCl particles coated with stearic acid had an average value of 0.25,

indicating a significantly lower loss rate for H_2SO_4 onto an aerosol with a hydrocarbon film.

The mass accommodation coefficients measured for H_2SO_4 loss onto NaCl and $(NH_4)_2SO_4$ aerosol in this study are similar and fall within the uncertainty range of either measured value. The relative humidity of the flow gas in these experiments was well below the deliquescence point of both salts so that the uptake likely represents a physical adsorption of H_2SO_4 onto a partially hydrated crystalline salt surface (Ewing and Peters, 1997). The similarity in the two surfaces with respect to H_2SO_4 adsorption is evident from the small difference in α for the salts. No appreciable trend in α with relative humidity was observed. However, over our limited range of 0.3 to 11 % RH, the change in α due to variation in H_2O coverage of the aerosol surface and/or the degree to which H_2SO_4 is hydrated in the gas phase is expected to be too small to be measurable in the present study.

The value of α found for a NaCl aerosol coated with stearic acid was approximately a factor of three smaller than that measured for the bare aerosol. Stearic acid is a long chain carboxylic acid ($CH_3(CH_2)_{16}COOH$) that is insoluble in water and consequently is expected to form a film on the aerosol surface. Figure 4 shows the aerosol size distribution for bare NaCl particles and NaCl particles with thick and thin coatings of stearic acid. The acid coverage was at least several nanometers, indicating that the surface was completely coated with one or more monolayers for both coating levels. The aerosol with the higher coverage of stearic acid resulted in a faster loss rate of H_2SO_4 and thus a larger value for α ;α = 0.31 and 0.19 for high and low stearic acid coverage, respectively. This difference

between high and low coverage could be due to a change in the orientation of the acid on the aerosol surface leading to a concomitant change in the number of polar binding sites available for H_2SO_4. Alternatively, the aerosol surface with the higher stearic acid coverage may have been highly irregular, resulting in a higher aerosol surface area. Certainly more knowledge of the aerosol surface structure and a far more extensive set of uptake measurements are needed to understand H_2SO_4 loss rate onto aerosols containing organics.

Discussion of error

Error in the calculated value of α will arise from uncertainty in the diffusion coefficient, point to point variation in the aerosol surface area during a single decay, uncertainty in the measured aerosol surface area and changes in the H_2SO_4 vapor pressure with instabilities in the flow gas relative humidity. Changes in the value of D_g of $\pm$ 20% lead to only a 3 percent change in α. An uncertainty in α near 5 percent could be accounted for from the standard deviation in the averaged aerosol size distributions within a single experimental decay measurement. In contrast, the mass accommodation coefficient was very sensitive to changes in the H_2SO_4 vapor pressure with relative humidity. The vapor pressure of H_2SO_4 above a solution declines exponentially with increased relative humidity [Marti et al., 1997, Ayers et al. 1980]. In the dry flow gases of these experiments, a 0.1 percent change in the relative humidity in the flow gas from 1 to 1.1 % relative humidity could produce a change in the H_2SO_4 vapor pressure on the order of 3×10^7 molecule cm^{-3}, i.e. close to 15 percent of the concentration range of the signal decay. The H_2SO_4 signal was far less sensitive to changes in the water vapor pressure at a

relative humidity above 5 percent. Error arising from small variations in the flow gas relative humidity and aerosol size distribution is evident in the calculated fit of the signal to an exponential decay. As seen from Table 1, the uncertainties in the calculated values of α are highest in the decays with the lowest relative humidity. Ideally, we would have liked to supply a set level of gas phase H_2SO_4 that was not so severely limited by the flow gas relative humidity.

As a result of laminar flow and diffusion, the H_2SO_4 concentration will develop a parabolic profile across the flow tube. Owing to this radial gradient in H_2SO_4, the observed decay constant is a nonlinear function of the first order wall loss rate and the pseudo first order aerosol loss rate. In order to quantify the error introduced by our simplified analysis (which assumes the observed rate constant is a linear sum of k_1 and k_d) , k_1 was determined using the method of Brown [1978], modified for species detection in a central cross section of the laminar flow. The calculated values of α using this method were within 3 percent of those values calculated using the measured flow time from equation 1. The standard errors of the average in both methods were the same. Here, the radial gradients in the flow time and H_2SO_4 concentration across the sampled region were small enough that the observed rate constant, K, could be considered a linear sum of k_1 and k_d.

Error in the value of α will arise also from uncertainty in the SEMS measurements of the aerosol size distribution and calculated particle surface area. Most of this uncertainty is associated with accuracy in the pressure, flow rates, dilution of the sample gas, transmission of the particles through the DMA, the particle charging probabilities and the

inversion algorithm used to characterize the particle size distribution. We estimate the sum of the uncertainties in these parameters to be approximately 25 % of the calculated particle surface area. The reported uncertainties in the average values of α for loss of H_2SO_4 onto NaCl and $(NH_4)_2SO_4$ particles is a sum of the 25% systematic error associated with the uncertainty in the aerosol surface area, a 3% error due to uncertainty in the H_2SO_4 diffusion coefficient, a 3% error in the flowtime measaurement and twice the standard error (2σ).

Atmospheric Implications

Under the ambient conditions of the lower troposphere, the composition and phase of submicron particles depend on the local sources of condensable gases and the relative humidity. The fine-mode particles in a remote marine environment are primarily aqueous solutions of sulfate, methyl sulfonate and ammonium ions [Heubert et al., Savoie et al.] In addition to sulfate and ammonium ions, aerosols in continental air masses may contain nitrate ions and as much as 20 - 50% by mass organic molecules [Novokov and Penner, 1993, Saxena et al.,1996]. Also, gas phase sulfuric acid will be hydrated with one or more H_2O molecules almost entirely throughout the lower troposphere [Kumala et al., 1991, Marti et al.,1996].

We can expect the uptake rate of H_2SO_4 onto particles to vary with the level of H_2SO_4 hydration and the particle composition. Although these experiments were conducted well below the deliquescence point of NaCl (75% RH) and $(NH_4)_2SO_4$ (80% RH) the aerosol surfaces likely had some H_2O coverage. Studies of H_2O adsorption

isotherms on NaCl crystallites by Barraclough and Hall [1974] indicate that a NaCl crystallite surface has < 0.1 to 0.5 monolayer of H_2O coverage over the relative humidity range of the present experiments. A recent series of papers [Ewing and Peters, 1997, Allen et al.,1996, J.M.Laux et al., 1994, Beichert and Finlayson-Pitts, 1996] have explored the role of surface morphology in both H_2O adsorption and H_2O mediated adsorption of HNO_3 to a NaCl surface. Studies of H_2O adsorption on NaCl [Ewing and Peters, 1997] found H_2O coverage to increase with surface defects and proposed that the binding energy of H_2O to a rough surface was greater than that of a smooth surface. In their study of the reactive uptake of HNO_3 onto NaCl particles, Beichert and Finlayson-Pitts [1996] noted that the presence of a surface adsorbed water layer played a critical role in the uptake of HNO_3 by providing a polar binding site and medium to solvate the acid on the salt surface. Here too, surface defects were found to be necessary in H_2O and HNO_3 adsorption. The small difference in the mass accommodation coefficients of H_2SO_4 for $(NH_4)_2SO_4$ and NaCl particle surfaces of the present study indicates either a similarity in the number of surface defects on these two salt particles or that the uptake of H_2SO_4 onto the aerosols was relatively indifferent to presence of surface defects on the salt surface. Also no trend in the mass accommodation coefficient over the range in relative humidity from 0.3 and 11 percent was observed, indicating that H_2O may not have a critical role in the initial adsorption of H_2SO_4 onto the particle surface. In the case of H_2SO_4 uptake onto a neutral salt, the binding energy of H_2SO_4 appears sufficiently strong enough that the acid readily adsorbed to the salt surface and further enhancement of the uptake rate by surface defects or water had little effect on an already high mass accommodation coefficient.

The uptake of H_2SO_4 onto ambient aerosol droplets involves the adsorption and subsequent solvation of H_2SO_4 into the aqueous droplet. Here, the energetics of solvation and hence reevaporation rate of H_2SO_4 depends on the Henry's law constant which varies with the particle composition, pH and temperature. The vapor pressure of H_2SO_4 above a mixed sulfate aerosol (i.e.,a sulfuric acid / ammonium sulfate solution) was found to increase with the percent H_2SO_4 composition of the aerosol [Marti et al., 1997]. Thus, the accommodation coefficient is expected to decrease with particle acidity.

As evident in the observed decrease in α for an aerosol coated with stearic acid, the initial adsorption of H_2SO_4 varies with the aerosol surface composition. As an oxidizing agent, H_2SO_4 may react chemically with organics present in the aerosol leading to increased adsorption of H_2SO_4 onto aerosols. Our initial attempt at coating the aerosols with stearic acid involved solvating the stearic acid in ethanol or propanol. However, we found these alcohols readily reacted with H_2SO_4 to form organic-sulfate clusters which completely depleted the HSO_4^- signal. This serendipitous discovery may indicate that H_2SO_4 reacts with atmospheric organics, either in the gas phase or in aerosol solutions.

The measured mass accommodation coefficients for NaCl and $(NH_4)_2SO_4$ aerosol may coincide well with the loss rate of H_2SO_4 onto neutral salt aerosols found in a remote marine environment. However, evidence from the reduced loss rate of H_2SO_4 on to an aerosol coated with an organic film and a previous experiment which found the H_2SO_4 vapor pressure above an aerosol to increase with aerosol acidity [Marti et al., 1997] suggests the H_2SO_4 mass accommodation coefficient varies broadly with the particle composition. A previous experiment by Van Dingenen and Raes [1991] measured a value

for α between 0.02 and 0.09 for loss of H_2SO_4 onto aqueous sulfate aerosol where the aerosol composition most closely resembled that of stratospheric aerosol. Alternatively, field measurements at a remote continental site which measured steady state H_2SO_4 production and loss rates found good agreement with their data using a value of α of 0.5 and 1.0 [Tanner and Eisele,1993, Weber et al.,1996]. In these two field studies the aerosol likely had a mixed aqueous composition of SO_4^{2-}, NO_3^-, NH_4^+, inorganic metal and organic ions.

Conclusion

In this study direct measurements were made of the H_2SO_4 loss rate onto submicron aerosols for three different aerosol substrates. The mass accommodation coefficients were calculated from the first order rate constants and were found to be 0.73 ± 0.21 and 0.80 ± 0.23 for H_2SO_4 loss onto $(NH)_4SO_4$ and NaCl aerosols, respectively. The loss rate of H_2SO_4 on to a NaCl aerosol coated with stearic acid was lower than that of the salt aerosol with measured values of the mass accommodation coefficient of 0.31 and 0.19 for high and low stearic acid coverage, respectively.

The values of α are considerably higher than previous measurements of H_2SO_4 uptake onto aqueous H_2SO_4 droplets [Van Dingenen and Raes, 1991], but compare well with the value of $\alpha = 0.5$ to 1.0 deduced from the results of a field study of steady state production and loss rates of H_2SO_4 at a remote continental site [Tanner and Eisele,1993, Weber et al.,1996]. The higher values of α will result in higher calculated aerosol growth rates. In steady state model calculations of aerosol formation and growth, a higher aerosol growth

rate would mean lower estimates of the gas phase H_2SO_4 concentration and consequently slower aerosol nucleation rates.

The uptake of H_2SO_4 was found to depend strongly on the aerosol composition, with a lower value of α reported for an aerosol with an organic coating. A similar reduction in α has been observed for uptake of NH_3 onto aerosol with an organic coating [Däumer et al., 1992]. The variability in α with aerosol composition suggests that model evaluations of aerosol nucleation and growth need to consider the regional aerosol composition. In their model study, Kerminen and Wexler [1995] proposed using a value of α that decreases with increased aerosol size because they proposed that larger particles may have a higher organic composition and therefore a slower H_2SO_4 uptake. However, the chemical reactivity of H_2SO_4 with organics may affect their uptake onto aerosols such that α may vary with the specific organic compounds present in the aerosol.

Further studies of H_2SO_4 uptake onto aerosols indicative of the lower troposphere are needed to improve our understanding of aerosol growth and H_2SO_4 loss rates. Studies of the uptake rate of H_2SO_4 onto an aerosol surface of varying organic composition as well as aerosol pH, temperature and relative humidity would enhance the ability of model calculations to predict aerosol formation and growth rates over a range of diverse atmospheres.

Acknowledgments

The authors wish to thank David Tanner for his expertise and help with the CIMS instrumentation as well as Steve Ball and Lee Mauldin for their helpful comments. This

work was supported by NASA grant NASA/NAGW-3751 and 4692. R.Weber gratefully acknowledges support by the Department of Energy under contract DE-ACO2-76CH00016 as part of the Atmospheric Chemistry Program within the Office of Health and Environmental Research.

References

Allen, H.C., J.M.Laux, R.Vogt, B.J. Finlayson-Pitts and J.C. Hemminger, Water-induced reorganization of ultrathin nitrate films on NaCl: implications for the tropospheric chemistry of sea salt particles, *J. Phys. Chem., 100*, 6371-6375, 1996.

Ayers, G.P., R.W. Gillett and J.L. Gras, On the vapor pressure of sulfuric acid, *Geophys. Res. Lett., 7*, 433-436, 1980.

Barraclough, P.B. and P.G. Hall, Adsorption of water vapor by lithium fluoride, sodium fluoride and sodium chloride, *Surface Science, 46*, 393, 1974.

Beichert, P. and B.J. Finlayson-Pitts, Knudsen cell studies of the uptake of gaseous HNO_3 and other oxides of nitrogen on solid NaCl: the role of surface-adsorbed water, *J. Phys. Chem., 100*, 15218-15228, 1996.

Brown, R.L., Tubular flow reactors with first order kinetics, *J.Res. Nat. Bureau Standards, 83*, 1-8, 1978.

Dahneke, B.E., *Aerosol Sci., 4*, 139, 1973.

Däumer, B., R.Niessner and D.Klockow, Laboratory studies of the influence of thin organic films on the neutralization reaction of H_2SO_4 aerosol with ammonia, *J. Aerosol Sci.*, 23, 315-325, 1992.

Eisele, F.L. and D.J.Tanner, Ion-assisted tropospheric OH measurements, *J. Geophys. Res., 96*, 9295, 1991.

Eisele, F.L. and D.J. Tanner, Measurement of the gas phase concentration of H_2SO_4 and methane sulfonic acid and estimates of H_2SO_4 production and loss in the atmosphere, *J.Geophys. Res., 98*, 9001-9010, 1993.

Ewing, G.E. and S.J. Peters, Adsorption of water on NaCl, *Surface Reviews and Letters*, accepted 1997.

Fuchs, N.A. and A.G. Sutugin, Highly Dispersed Aerosols, pp. 47-60, Ann Arbor Science, Ann Arbor, Michigan, 1970.

Hagan, D. E. and D.J. Alofs, Linear inversion method to obtain aerosol size distributions from measurements with a differential mobility analyzer, *Aerosol Sci. Technol., 2,* 465-475, 1983.

Heubert, B.J., L. Zhuang, S. Howell, K. Noone, and B. Noone, Sulfate, nitrate, methanesulfonate, chloride, ammonium, and sodium measurements from ship, island, and aircraft during the Atlantic Stratocumulus Transition Experiment / Marine Aerosol Gas Exchange, *J. Geophys. Res., 101,* 4413-4423, 1996.

Kelly, W.P. and P.H. McMurry, Measurement of particle density by inertial classification of differential mobility analyzer-generated monodisperse aerosols, *Aerosol Sci. Technol., 17,* 199, 1992.

Kerminen, V.M.and A.S. Wexler, Enhanced formation and development of sulfate particles due to marine boundary layer circulation, *J. Geophys. Res., 100,* 23051-23062, 1995.

Kriedenweis, S.M., J. Penner, F. Yin, and J.H. Seinfeld, The effects of dimethylsulfide upon marine aerosol concentrations, *Atmos. Environ., 25A,* 2501-2511,1991.

Kulmala, M., V.M. Kerminen, and A. Laaksonen, Simulations on the effect of sulfuric acid formation on atmospheric aerosol concentrations, *Atmos. Environ., 29,* 377-382, 1995.

Kulmala, M., M. Lazaridis, A. Laaksonen, and T. Vesala, Extended hydrates interaction model: hydrate formation and the energetics of binary homogeneous nucleation, *J. Chem. Phys., 94,* 7411-7413, 1991.

Lodge, J.P. and B.J. Tufts, An electron microscope study of sodium chloride particles as used in aerosol generation, *J.Colloid. Sci., 10,* 256, 1955.

Marti, J.J., A. Jefferson, X.P. Cai, C. Richert, P.H. McMurry, and F.L. Eisele, The H_2SO_4 vapor pressure above sulfuric acid and ammonium sulfate solutions, *J. Geophys. Res.*, accepted 1996.

Novakov, T. and J.E. Penner, Large contribution of organic aerosols to cloud-condensation nuclei concentrations, *Nature, 365,* 823-826, 1993.

Pandis, S.N., L.M. Russell, and J.H. Seinfeld, The relationship between DMS flux and CCN concentration in remote marine regions, *J. Geophys. Res., 99,* 16945-16957,1994.

Penner, J., T.M.L. Wigley, P. Jaumann, B.D. Santer, and K.E. Taylor, Anthropogenic aerosols and climate change: a method for calibrating forcing, *Assessing Climate Change: The Story of the Model Evaluation*, The Consortium for Climate Assessment, submitted, 1996.

Roedel, W. Measurements of sulfuric acid saturation vapor pressure: implications for aerosol formation by heteromolecular nucleation, *J. Aerosol Science, 10,* 375-386, 1979.

Savoie, D.L., J.M. Prospero, R.J. Larsen, F. Huang, M.A. Izaguirre, T. Huang, T.H. Snowdon, L. Custals, and C.G. Sanderson, Nitrogen and sulfur species in Antarctic aerosols at Mawson, Palmer Station, and Marsh(King George Island), *J. Atmos. Chem., 17,* 95-122, 1993.

Saxena, P.and L.M. Hildemann, Water-soluble organics in atmospheric particles: a critical review of the literature and application of thermodynamics to identify candidate compounds, *J. Atmos. Chem., 24,* 57-109, 1996.

Schwartz, S., The whitehouse effect - shortwave radiative forcing of climate by anthropogenic aerosols: an overview, *J. Aerosol. Sci., 27,* 359-382,1996.

Tanner, D.J. and F.L. Eisele, Present OH measurement limits and associated uncertainties, *J. Geophys. Res., 100,* 2883- 2892, 1995.

Tanner, D.J., A.Jefferson and F.L. Eisele, Selected ion chemical ionization mass spectrometric measurement of OH, *J.Geophys. Res.,* accepted 1996.

Van Dingenen, R.and F. Raes, Determination of the condensation accommodation coefficient of sulfuric acid on water-sulfuric acid aerosol, *Aerosol Sci. and Tech., 15,* 93-106,1991.

Wang, S.C. and R.C. Flagan, Scanning electrical mobitity spectrometer, *Aerosol Sci. Technol., 13,* 230-240, 1990.

Weber, R.J., Measurements of new particle formation and ultrafine particle growth rates at a clean continental site, *J. Geophys. Res.,* (submitted, 1996).

Wigley, T.M.L. and S.C.B. Raper, Implications for climate and sea level of revised IPCC emissions scenarios, *Nature, 357,* 293-300, 1992.

Figures

Figure 1. Diagram of flow tube kinetic reaction cell, aerosol generation and detection and CIMS instrument.

Figure 2. Measured ion residence time in the flow tube as a function of injector position. A linear fit of the measured values gives a flow time of time(sec) = 0.0639 x(cm) + 0.3515. The bold line is the calculated residence time assuming laminar flow and an 18% sampling of the central flow tube area. The residence time offset in the measured flow rate reflects the time for an ion to travel from an arbitrary zero point on the flow tube to the CIMS detector.

Figure 3. The relative H_2SO_4 signal vs. injector position under conditions of a) no aerosol present, b) an aerosol surface area of 3.0×10^{-6} cm^2 cm^{-3} and c) an aerosol surface area of 8.8×10^{-6} cm^2 cm^{-3}.

Figure 4. NaCl aerosol size distributions with no stearic acid (triangles), low stearic acid (diamonds) and high stearic acid coverage (circles).

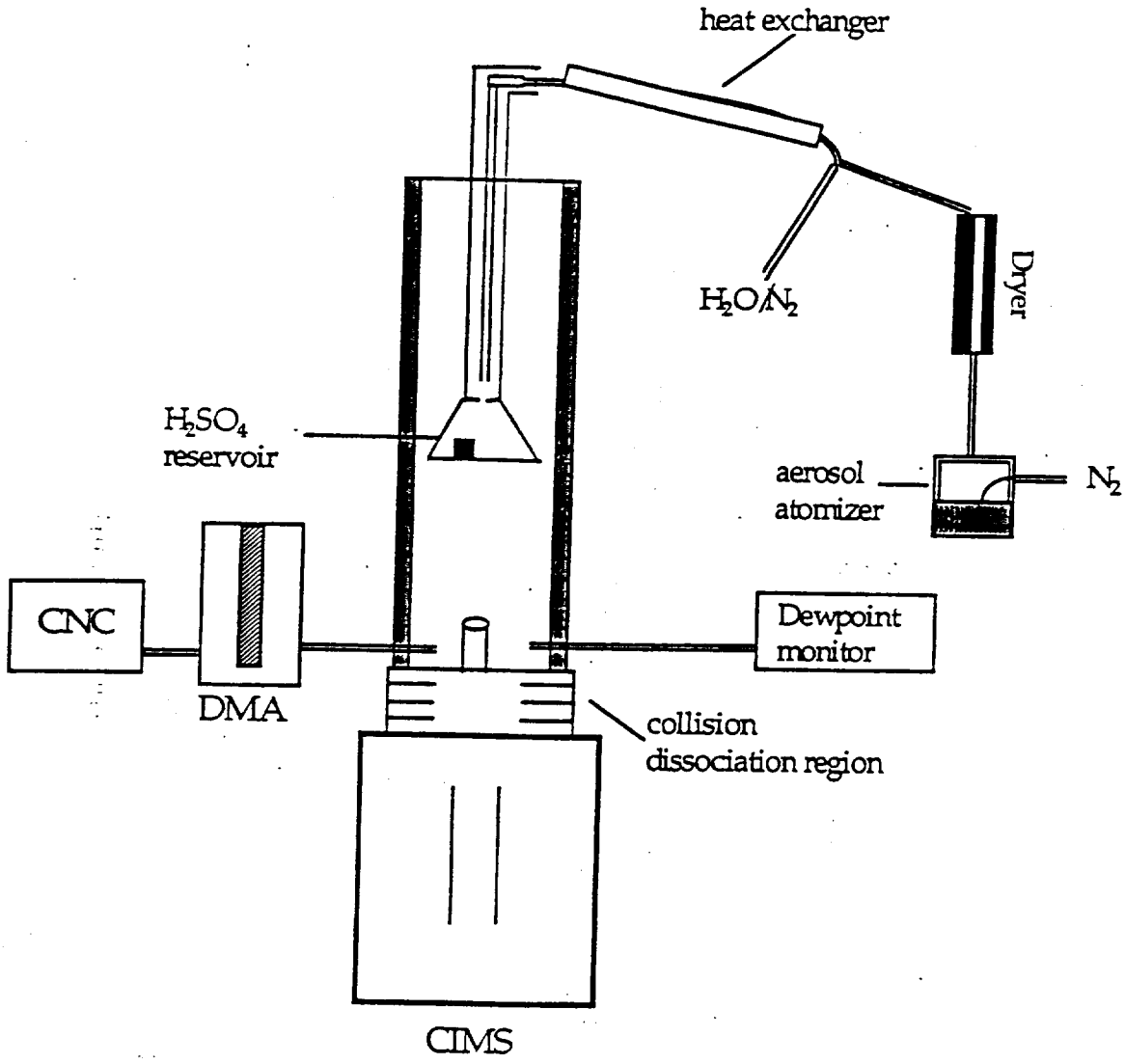
heat exchanger
H_2O/N_2
Dryer
H_2SO_4
reservoir
aerosol
atomizer
N_2
CNC
DMA
Dewpoint
monitor
collision
dissociation region
CIMS

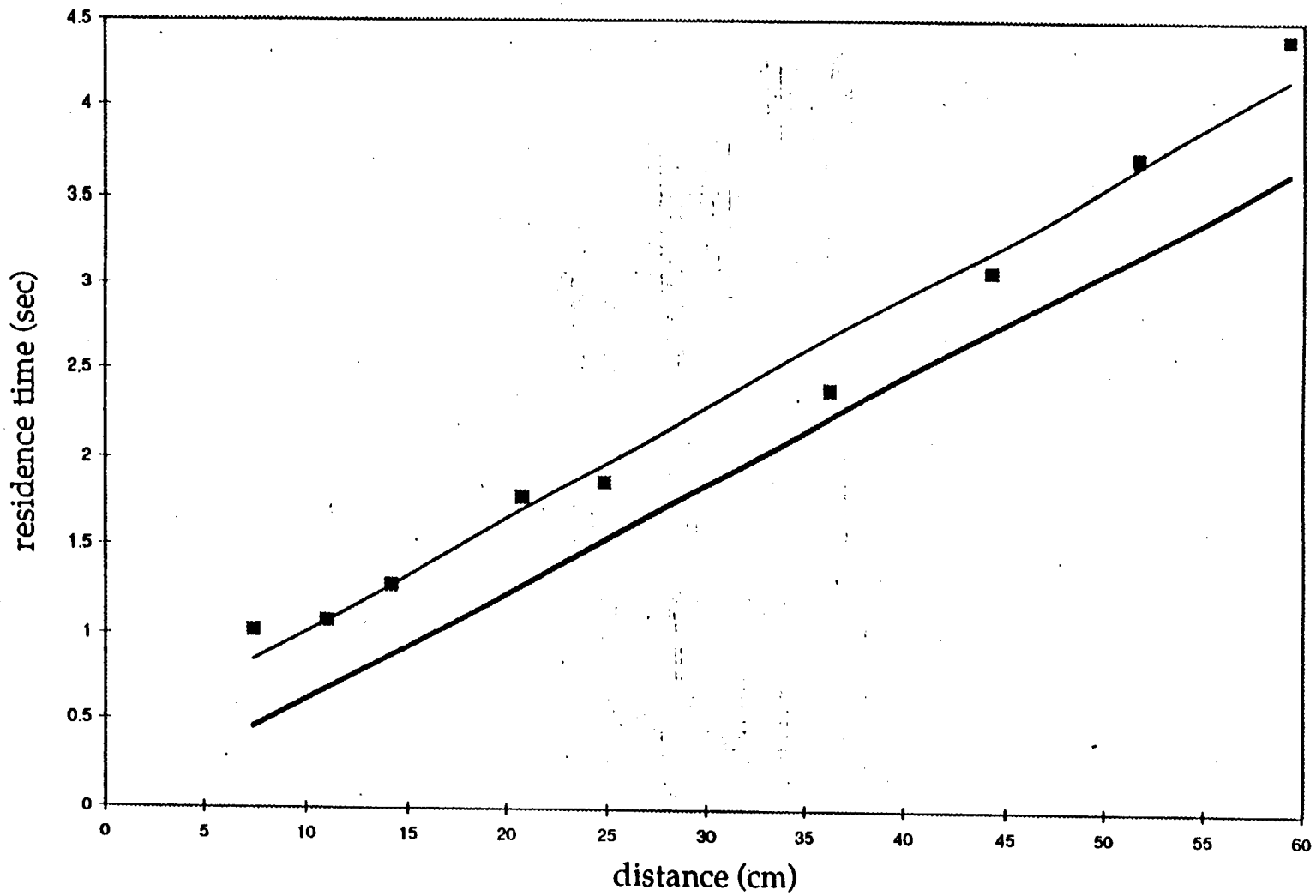
residence time (sec)
4.5
4
3.5
3
2.5
2
1.5
1
0.5
0
0
5
10
15
20
25
30
35
40
45
50
55
60
distance (cm)

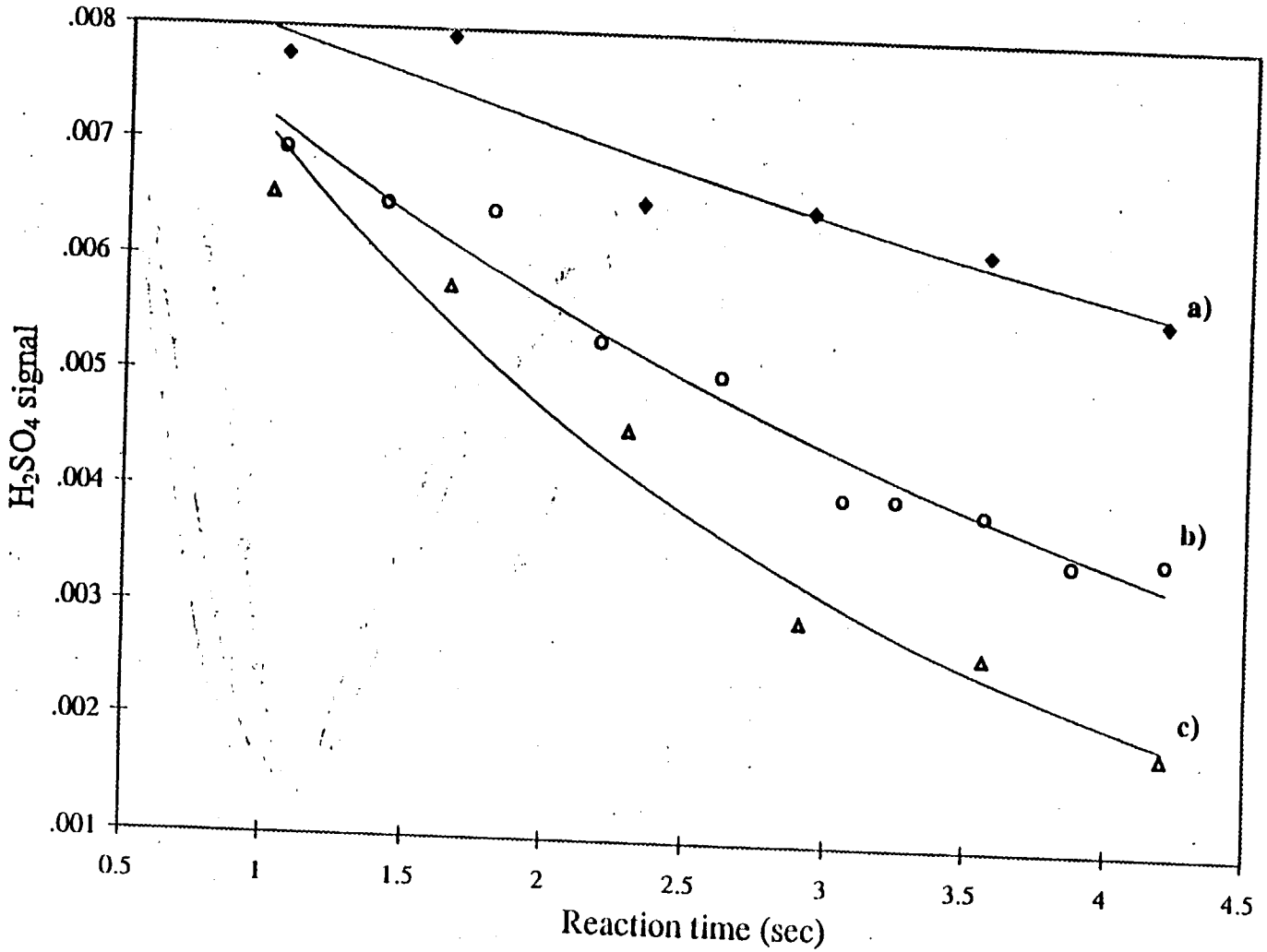
.008
.007
.006
.005
.004
.003
.002
.001
H_2SO_4 signal
0.5
1
1.5
2
2.5
3
3.5
4
4.5
Reaction time (sec)
a)
b)
c)

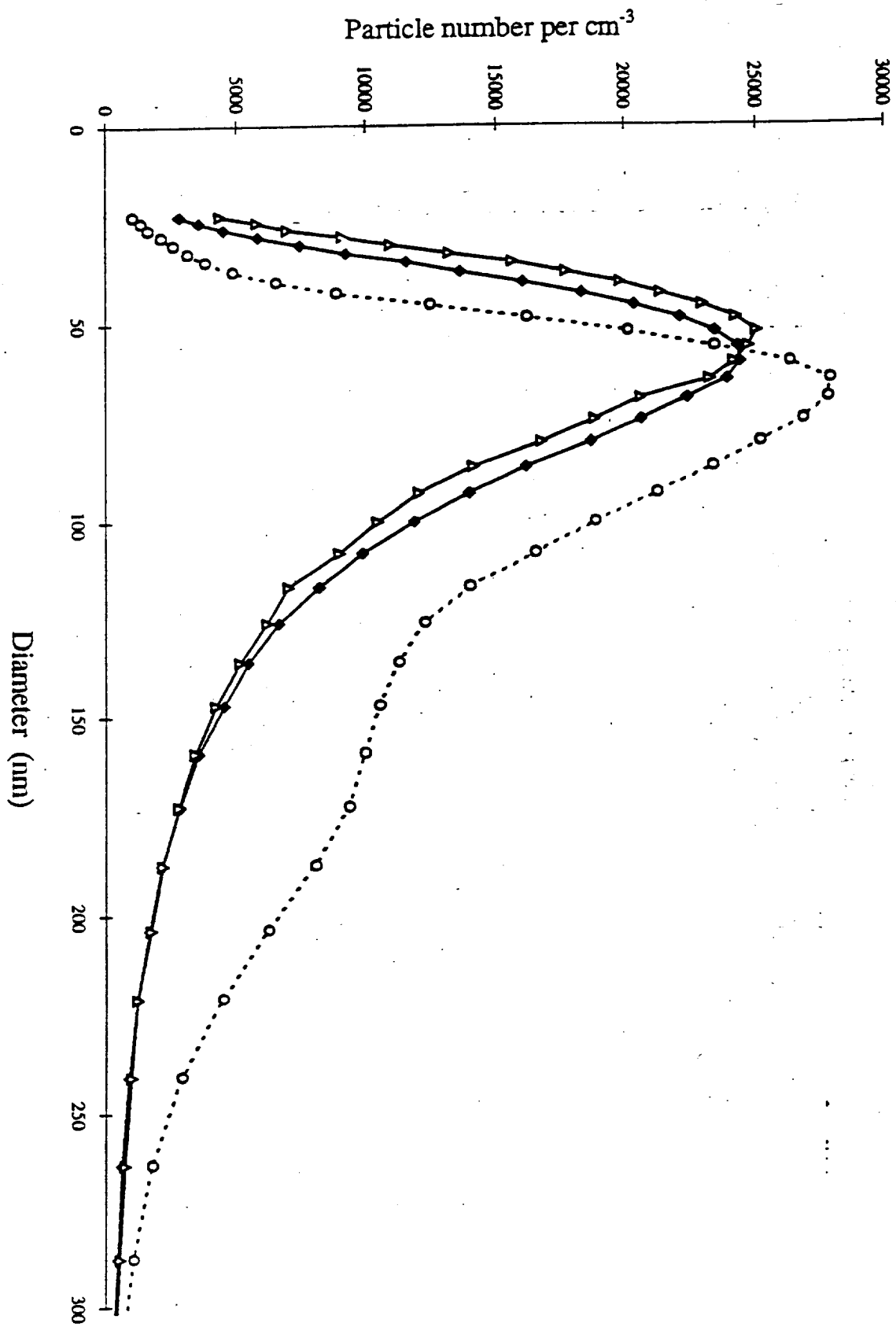
Particle number per cm-3
0
5000
10000
15000
20000
25000
30000
Diameter (nm)
0
50
100
150
200
250
300

TABLE 1. Summary of Measured 1st Order Rate Constants and Mass Accommodation Coefficients

Aerosol	RH, %	k_1, s^{-1}	α	uncertainty
NaCl	1.6	0.378	0.62	0.20
	0.3	0.139	0.85	0.30
	1.7	0.136	0.78	0.25
	1.4	0.169	0.96	0.34
	11.0	0.391	0.91	0.26
	5.2	0.341	0.70	0.21
$(NH_4)_2SO_4$	1.9	0.383	0.75	0.22
	5.2	0.327	0.80	0.26
	0.5	0.250	0.64	0.37
Stearic acid	5.4	0.241	0.31	0.08
	4.4	0.086	0.19	0.06